

# **Widespread inhibition proportional to excitation controls the gain of a leech behavioral circuit**

## ***Authors***

Baca, Serapio M.\*  
Marin-Burgin, Antonia\*  
Wagenaar, Daniel A.\*  
Kristan Jr., William B.

\*these three authors contributed equally to this work

## ***Authors addresses***

Section of Neurobiology,  
Division of Biological Sciences  
University of California, San Diego  
La Jolla, CA 92093-0357

## ***Corresponding author***

### **William B. Kristan, Jr.**

Section of Neurobiology,  
Division of Biological Sciences  
University of California, San Diego  
La Jolla, CA 92093-0357  
**wkristan@ucsd.edu**

***Keywords:*** imaging, invertebrates, Voltage-sensitive dyes, behavior, motor circuit, sensory-motor

***Characters with spaces:*** 43,779 (text)  
15,126 (legends)  
11,278 (references)

***Number of Figures:*** 8

## **SUMMARY**

Changing gain in a neuronal system has important functional consequences, but the underlying mechanisms have been elusive. Models have suggested a variety of neuronal and systems properties to accomplish gain control. Here, we show that the gain of the neuronal network underlying local bending behavior in leeches depends on widespread inhibition. Using behavioral analysis, intracellular recordings, and voltage-sensitive dye imaging, we compared the effects of blocking just the known lateral inhibition with blocking all GABAergic inhibition. This revealed an additional source of inhibition, which was widespread and increased in proportion to increasing stimulus intensity. In a model of the input/output functions of the three-layered local bending network, we showed that inhibiting all interneurons in proportion to the stimulus strength produces the experimentally observed change in gain. This relatively simple mechanism for controlling behavioral gain could be prevalent in vertebrate as well as invertebrate nervous systems.

***Running title:*** Gain control by inhibition

## INTRODUCTION

Behaviors result from an interplay between excitation and inhibition within the nervous system. Classically, two functions for inhibition were recognized: reciprocal inhibition, with one behavior being inhibited while another is expressed ; and lateral inhibition, the shutting down of sensory pathways just outside the area being stimulated, which serves to sharpen the perception of the stimulus . In recent years, a new form of interaction has been described, namely simultaneous excitation and inhibition , which has been found in many parts of the vertebrate nervous system , including the spinal cord . Several functions have been suggested for this balanced excitation and inhibition, including the production of response variability and the control of spike transmission through the thalamus to the cortex . A recent intriguing possibility is that the balance between excitation and inhibition onto a neuron affects the gain of its response to a given input, because the conductance of the neuron can vary dramatically without changing the membrane potential . The issue of gain control has attracted recent attention for its importance in sensory and motor processing as well as its likely role in such higher functions as attention , for the coordinate transformations required for visually guided reaching movements , and for object recognition in different areas of the visual field .

We wanted to know whether interactions between excitation and inhibition triggered by sensory stimulation in a feed-forward network can adjust the gain of a behavioral circuit. To approach this question, we studied how inhibition affects the amplitude of a simple reflexive response—local bending—in the medicinal leech, a response that is elicited by a localized touch and is produced by longitudinal muscle contraction on the side of the touch and relaxation of the corresponding muscles on the opposite side . The response varies with both touch location and touch intensity . The circuit that generates local bending involves a small number of identified sensory neurons , interneurons , and motor neurons . The only identified central inhibition in this circuit is provided by the connections from the inhibitory motor

neurons onto the excitatory motor neurons (Fig. 1). These inhibitors release GABA in a graded, spike-independent manner centrally onto the contralateral excitors and peripherally onto longitudinal muscle fibers. The connections were thought to produce an effective lateral inhibition that focused the excitation at the site of the touch and relaxed the opposite side, to produce the bend.

This circuit is an appropriate one to study gain control for several reasons. First, at a behavioral level, mechanical stimuli of increasing magnitude produce increasingly large responses. Second, the underlying circuit is a 3-layered, feed-forward network composed of a small number of identified neurons. Third, perturbing the activity of any of the individual neurons affects the expression of the behavior, thereby showing the behavioral significance of each neuron. Fourth, local bending depends on a population of distributed interconnections that include inhibitory connections.

We performed behavioral experiments while recording from neurons with intracellular microelectrodes and voltage-sensitive dyes. We monitored the activity of many motor neurons at once while knocking out inhibition both pharmacologically and electrophysiologically. We found that GABAergic inhibition among the motor neurons produced both lateral inhibition, as previously shown, as well as a generalized inhibition of most neurons in the CNS. This generalized inhibition was responsible for setting the gain of the response, which provided the broad dynamic range of the response to different levels of sensory stimulation. These results show that very localized sensory stimulation of the leech's skin produces a balanced excitation and inhibition that sets the gain of the response. The experiments and modeling suggest that this inhibition is strong and uniform across all interneurons, and possibly all motor neurons, in the ganglion.

## RESULTS

### **Role of GABAergic inhibition on local bending.**

To establish the input-output function for local bending at a given stimulus site, we used a loosely-pinned, flattened body wall preparation that was innervated by a single ganglion (Fig. 1B). To induce local bends, we applied tactile pulses of constant force to the skin for 3 seconds and used an optic flow algorithm to measure the resulting body movements along four lines of longitudinal markers at 0.5 sec after releasing the stimulus. We applied stimuli to the middle of either the right or left ventral surface (i.e., half-way between the ventral midline and the lateral edge) because previous studies have shown that these sites produced easily distinguishable bend profiles in body wall preparations. For each of 10 leeches, we applied 2 or 3 stimuli at each of 10 force levels between 0.75 and 400 mN. We then washed in a solution of 0.1 mM bicuculline methiodide (BMI). Access of BMI to the ganglion was ensured by applying it from below the pinned-out body wall through an inlet built into the Sylgard substrate. In pilot experiments, the effect of BMI was robust within 10 minutes, so we waited 10 minutes after application of BMI before repeating the stimulation protocol.

In control conditions, each touch produced a longitudinal contraction of the on-target ventral body wall at all intensities used, accompanied by relaxation of the off-target ventral, lateral, and dorsal body wall locations (Fig. 2 A-D, filled circles). The responses in all four locations were well fit by sigmoid curves (solid lines). The on-target responses were contractions that increased in amplitude with increasing stimulus intensity, plateauing at about 0.8 annuli of shortening. The off-target responses were, on average, relaxations whose amplitudes saturated at  $-0.4$  (Fig. 2B),  $-0.7$  (Fig. 2C), and  $-0.8$  (Fig. 2D) annuli in ventral, lateral, and dorsal locations.

Bath application of BMI greatly increased the magnitude of the on-target contractions, even at low force levels (Fig. 2A, open circles), and decreased the relaxations at the three off-target sites (Fig. 2B-D, open circles). In fact, the relaxations observed at the off-target ventral site in control conditions became contractions in the presence of BMI (Fig. 2B). To measure the size of the change induced by BMI, we multiplied the sigmoid curve obtained for the control responses by a value that made its plateau value equal to the sigmoid obtained in BMI. The multiplier values required were 2.1 (Fig. 2A), -1.0 (Fig. 2B), 0.2 (Fig. 2C), and 0.8 (Fig. 2D). These scaled values are shown as solid grey lines in Fig. 2A-D. The fact that the scaled curves were within one standard error of the observed data at every stimulus intensity at all four locations indicates that BMI increases the amplitude of the response uniformly over the whole range of stimulus intensities. In other words, the inhibition blocked by BMI changes the gain of the whole system.

To determine whether the BMI was having its major effects on the central nervous system or at the inhibitory connections onto the muscles (Stuart, 1970), we used a split body wall preparation (Fig. 3A) with a Vaseline well built around the ganglion. We applied BMI either to the ganglion inside the Vaseline chamber or to the body wall outside the chamber. The results to BMI application at the two locations were very distinct (Fig. 3): applying BMI to the body wall alone did not affect either the on-target or the off-target responses (even with 1.0 mM BMI), but applying 0.1 mM BMI to the ganglion produced a larger contraction at both sites, both in individual (Fig. 3A) and averaged responses (Fig. 3B). In fact, the on-target and off-target responses were not significantly different in the presence of BMI. This experiment leads to two conclusions: (1) the increased magnitudes of the local bending responses produced by BMI on the body wall (Fig. 2) were due entirely to blocking inhibition within the ganglion; and (2) the contribution of peripheral inhibition to local bending responses were unaffected by bath application of BMI.

Why BMI did not affect inhibition within the body wall might have three causes: (1) the BMI might not gain access to the neuromuscular junctions; (2) the GABA receptors on the muscles might be insensitive to BMI; or (3) the inhibitory terminals on muscles might be non-GABAergic. Whatever the cause, however, the non-blocked peripheral inhibition is the most likely explanation for the residual relaxation seen at lateral and dorsal body wall sites (Fig. 2C, D).

### **Hyperpolarizing the inhibitors broadens the local bending response.**

From previous studies, the known local bend circuitry in each segment is a 3-layered, feed-forward circuit consisting of just 4 sensory neurons (pressure sensitive P cells), about two dozen local bend interneurons (LBIs) and about the same number of longitudinal motor neurons (Fig. 4A). All the connections indicated are excitatory chemical connections except for the connections from the inhibitory motor neurons (DI and VI) onto the corresponding excitatory motor neurons (DE and VE); these are GABAergic inhibitory connections (Cline, 1986). To evaluate whether BMI exerted its effects by blocking these known inhibitory connections, we removed this inhibition from the circuit reversibly by strongly hyperpolarizing one of them. This is an effective procedure because all the inhibitory motor neurons are strongly electrically coupled to one another (Fig. 4B). We stimulated the skin while hyperpolarizing the inhibitor DI-1 throughout the local bend response, using a *hole-in-the-wall preparation* (Fig. 4C). In this example, the off-target response increased while the inhibitors were hyperpolarized but the amplitude of the on-target response did not change. Statistical comparisons of responses from 10 preparations (Fig. 4D) showed that the off-target increase was significant, and that the on-target responses were not different. This result shows that the central connections of the inhibitors onto the excitors functioned only to restrict the contraction to the side touched; in other words, the inhibitory connections among motor neurons produce lateral inhibition but do not contribute to the generalized inhibition.

## **Role of GABAergic inhibition on neuronal responses.**

### *Effects on motor neurons.*

To determine how generalized inhibition affects the central nervous system, we recorded intracellularly from motor neurons while stimulating one of the four mechanosensory neurons that triggers local bending. Previous studies have shown that stimulating a single P cell excites the excitatory longitudinal motor neurons with their motor fields in the same area as the touch (i.e., the on-target excitators), inhibits the excitatory longitudinal motor neurons on the opposite side (the off-target excitators), and elicits a mixed response in excitators with intermediate movement fields (the intermediate excitators). We replicated these findings using both electrophysiological and imaging techniques (Fig. 5). We stimulated a single P cell at 10 Hz for 500 ms (comparable to delivering moderate mechanical stimuli to the body wall) and repeated this stimulus train once per second for 10 cycles, to produce a signal detectable by the voltage-sensitive dyes (VSDs). When, for example, we stimulated a  $P_v$  neuron—one of the two P cells that innervates ventral leech skin—the on-target VE-4 motor neuron was excited (Fig. 5D), the off-target DE-3 motor neuron was inhibited (Fig. 5A), and the two intermediate excitatory motor neurons (Figs. 5B, C) received smaller excitation than the on-target motor neuron. These same features were seen in all 7 cases tested, in both the electrophysiological and the VSD recordings. (Note that the cyclic membrane potential changes are captured in the VSD recordings, but the faster membrane potential shifts were lost because of the slow time constant of the dyes.)

We then stimulated the same neuron after changing the bathing solution to saline containing 0.1 mM BMI to block GABAergic inhibition. As in the behavioral experiments (Fig. 2), blocking GABAergic inhibition increased the excitation made by  $P_v$  onto all excitatory motor neurons (right-hand panels in Figs. 5A-D, with a light grey background): neurons that had received excitation in control conditions (5B,

D) received significantly larger excitation in the BMI saline, and those that had been inhibited were now excited. These effects of BMI were observed in all 7 preparations tested. These results show that increases in the behavioral responses induced by BMI (Fig. 2) are apparent in the responses of the excitatory motor neurons.

We were concerned that BMI application might produce an excitatory effect on neurons in the circuit, as has been seen in mammalian neurons (Seutin and Johnson, 1999). To control for such a direct effect of BMI on leech neurons, we applied 100  $\mu$ M BMI to isolated ganglia while monitoring the membrane potential and the input resistance of sensory neurons, interneurons, and motor neurons—both excitatory and inhibitory—in the local bend circuit. BMI application did not affect the membrane potential of mechanosensory P cells (they depolarized by  $0.5 \pm 1.7$  mV,  $n=5$ ). BMI application slightly hyperpolarized interneurons and motorneurons: interneuron 212 hyperpolarized  $4.5 \pm 1.2$  mV ( $n=3$ ); excitatory motor neurons DE-3 and VE-4 hyperpolarized  $5.7 \pm 1.6$  mV ( $n=4$ ) and  $4.5 \pm 2.0$  mV ( $n=4$ ), respectively; and the inhibitory motor neurons DI-1 and VI-2 hyperpolarized  $5.4 \pm 1.5$  mV ( $n=4$ ) and  $5.3 \pm 0.9$  mV ( $n=3$ ), respectively. BMI did not produce any significant change ( $p > 0.05$ , t-Test) in the input resistance of any of these recorded neurons. Hence, the only direct effect of BMI onto the neurons in this circuit was inhibitory, an effect opposite to the generalized excitation seen in local bending after applying BMI. These results showed that the increased excitation in the network seen after BMI application, therefore, were not caused by direct excitatory effects of BMI on the neurons in the circuit.

### ***Effects on other neurons.***

Because we were imaging all the neurons visible on the dorsal surface of the ganglion with the VSDs while recording from the excitatory motor neurons electrophysiologically, we could also determine the activity of another 40-50 neurons (Fig. 6). In standard saline (left panels of Fig. 6), the intracellular

recordings (Fig. 6B) and the trajectories of the optical signals from the imaged neurons (Fig. 6C, D) show that many of them respond to each P cell spike burst, seen as oscillations at the same frequency as the stimulus bursts. Those that were phase-locked to the stimulus were active in different phases of the stimulus cycle. This phase-locking was quantified using polar plots (Fig. 6E) that show both the phases (distance around the circumference) and the coherence magnitudes (distance from the center) for all visible neurons. Neurons with significant coherence values (outside the dashed lines in Fig. 6E) have been colored in the ganglionic images (Fig. 6A) and in the individual trajectories (Fig. 6C). Brighter colors represent higher coherence values, and different hues represent the phases of the responses relative to the stimulus. The neurons that were phase-locked to the stimulated P<sub>v</sub> cell in normal saline clustered in two distinct phases (Fig. 6E), corresponding to excitation (clustered between 45° and 90°) and inhibition (scattered points around 180°).

We then repeated the same P<sub>v</sub> stimulation regime after replacing the bathing solution with saline containing 0.1 mM BMI (Fig. 6, middle panels). With all GABAergic inhibition blocked, every neuron had large amplitude, phase-locked oscillations in the VSD trajectories (Fig. 6C2, D2) that clustered around 90° (Fig. 6E2), indicating that the P<sub>v</sub> spike bursts now excited *all* the neurons. (The peak of the excitatory responses were, on average, more delayed in BMI than in control because the inhibition caused by each stimulus train occurred later than the excitation; therefore, blocking the inhibition selectively enhanced the later part of the excitatory response, which produced the observed delay in the peak excitation.) One example of a switch in the nature of the response is provided by the off-target cell DE-3 (arrow in Fig. 6E2), which switched its phase from 220° to 90°. This switch is also apparent in the intracellular recordings (Fig. 6B1, B2). Comparing the left and middle panels of Fig. 6 shows that approximately half the neurons were significantly coherent with the spike bursts in normal saline, with most of these being excited and the rest inhibited. After removing the GABAergic inhibition with BMI, the P<sub>v</sub> stimuli strongly

excited every neuron. We did not see consistent or large changes in the membrane potential or in the spontaneous activity of the neurons recorded intracellularly when BMI was added, indicating that the major changes in response patterns in BMI saline required sensory stimulation. The effects of BMI reversed within 10 minutes after washing the ganglion with normal saline (right panels of Fig. 6).

To be sure that the BMI did indeed block inhibition, we stimulated inhibitors through intracellular electrodes and found that BMI was very effective in blocking their central inhibitory effects on excitors (data not shown). Interestingly, many neurons that were clearly inhibited by the inhibitors in saline were found to be excited by them in the presence of BMI, possibly by their electrical connections. Such dual electrical and chemical connections between neurons have been observed in the leech CNS , as well as in other nervous systems .

It should be noted that included in the many neurons that were more strongly excited by Pv stimulation with BMI present were the inhibitory motor neurons. In fact, the inhibitors would be more strongly activated by Pv stimulation in the presence of BMI---because the central inhibition onto them would be blocked (Fig. 6) but their peripheral inhibition would not be affected (Fig. 3)---so that they would generate more relaxation of the muscles. Hence, the difference between the BMI and control curves in Fig. 2 is likely to be an underestimate of the effect of central inhibition.

### **Contribution of inhibitory motor neurons in the CNS expression of local bending.**

We determined whether the known inhibitory connections from inhibitors onto excitors contributed to the generalized inhibition by strongly hyperpolarizing one of them, in the same way that we had previously tested for the effects of this inhibition on local bending behavior (Fig. 4). For these experiments, we imaged the dorsal surface of each ganglion with VSDs while stimulating a P<sub>v</sub> cell before, during, and after hyperpolarization of the inhibitors (Fig. 7). In control recordings before and after

hyperpolarizing cell DI-1, the responses of the neurons to  $P_V$  stimulation (Fig. 7B1, B3) were comparable to the responses in Fig. 6D1 and D3: many neurons were excited (i.e., their activity phases were between  $0^\circ$  and  $90^\circ$ ) and a few were inhibited (phases were around  $270^\circ$ ). During cell DI-1 hyperpolarization, however,  $P_V$  stimulation no longer inhibited any neurons, and the excited neurons were more tightly clustered around  $45^\circ$  (Fig. 7C2). As indicated by the arrows in Fig. 6C1-3, hyperpolarizing the inhibitors inverted the response of the off-target excitors: normally inhibited by  $P_V$  stimulation, they were excited during hyperpolarization of the inhibitors in 6 of 6 experiments. However, hyperpolarizing the inhibitors did not produce an effect as widespread as that produced by BMI (compare Fig. 7B2 to Fig. 6D2), strengthening the conclusion that the central effects of the inhibitory motor neurons do not contribute to the generalized inhibition documented in Figs. 2 and 6.

The differences between application of BMI and hyperpolarizing the inhibitors are quantified in Fig. 7D. Application of BMI significantly increased the number of cells excited by  $P_V$  stimulation, measured as the number of neurons significantly coherent with the stimulus (one-way ANOVA,  $F_{3,33} = 12.11$ , a posteriori Tukey test  $P < 0.001$ ;  $n = 7$ ). Hyperpolarizing the inhibitor cell DI-1 did cause an increase in the number of neurons excited by  $P_V$  stimulation compared to control ( $P < 0.05$ ;  $n = 6, 7$ , respectively), but this number was less than the number excited by  $P_V$  stimulation during BMI application ( $P < 0.05$ ). The values for both conditions after treatment (BMI application or hyperpolarization) were not different from control.

### **A model with generalized feed-forward inhibition reproduced the major behavioral results.**

To test whether the observed generalized inhibition could change the gain of the output by acting on the interneurons, we modeled the input-output functions of the local bending circuit with and without the generalized inhibition, to mimic the effects of blocking inhibition with BMI (Fig. 8A). In particular,

we wanted to capture the two major features of the behavioral experiments (Fig. 2): (1) blocking the GABAergic inhibition caused a two-fold increase in the whole stimulus-response curve, whereas (2) the minimal touch intensity needed to cause a response did not change detectably. We used a simplified network model (Fig. 8A1), consisting of a mechanosensory P cell (P), which excites a local bend interneuron (LBI), which in turn excites a motor neuron (MN). The responses of the sensory neuron (curve P) provided the input to the circuit and the motor neuron responses (curves MN) were the output of the system. In the leech, there are approximately two dozen interneurons and motor neurons involved in the local bend reflex, so MN and I represent classes of neurons rather than single cells. To represent the generalized inhibition, we used a GABAergic cell (G), which is excited by the P cell and inhibits the interneuron with a synaptic strength  $\gamma$ . The firing rate of each cell is a simple sigmoidal function of its inputs, defined by only two parameters, a slope and a threshold. We examined the effect of the generalized GABAergic inhibition by varying the strength of the inhibitory synapses ( $\gamma$ ) onto the interneuron. In particular, setting  $\gamma = 0$  corresponds to complete blocking of GABAergic inhibition, corresponding to the application of BMI.

We chose connection strengths that produced an input/output function in the motor neuron that matched the behavioral data for the on-target region of the body wall (Fig. 2A); the responses of the P, G, LBI, and MN neurons in this condition are shown as black lines in the graphs in Fig. 8A2. With  $\gamma = 0$  (i.e., no inhibition), the responses of LBI and MN increased in amplitude but did not shift along the “Touch intensity” axis (dashed black lines). The model data closely matched the experimental data in control conditions (solid grey line) and after BMI application (dashed grey line). The gain of the model output could be controlled by altering the activation threshold of the GABAergic cell (thin black lines with triangle markers).

For GABAergic inhibition to result in a change of gain of the output, it was critical that the GABAergic cell (G) was activated over the same range of touch intensities as the P cell, and in the same manner. If, instead, the P-to-G synapse was so strong that the G-cell activity saturated at low touch intensities (Fig. 8B), the resulting G-cell activity was effectively constant over most of the P cell activity range, producing a left--right shift of the MN output along the "Touch intensity" axis (i.e., it had a subtractive effect) rather than a scaling (i.e., a multiplicative effect).

## DISCUSSION

We found that the circuit producing local bending behavior in the leech recruits two types of inhibition to produce a precise localized response: a lateral inhibition through inhibitory motor neurons that restricts the contraction to the side that was stimulated, and a generalized inhibition, independent of the inhibitory motor neurons, that restricts the amplitude of the response in proportion to the intensity of stimulation.

The generalized increase in the amplitude of local bending during BMI application (Fig. 2) was unexpected. The local bend circuit had been thought to be a broadly dispersed, feed-forward excitatory network from P cells to local bend interneurons, to motor neurons, with lateral inhibition only at the motor neuronal level to sharpen up the edges of the contraction and produce relaxation on the opposite side . Instead, the finding of a strong, generalized inhibition implies that the excitatory connections by themselves would produce a segment-wide contraction of all the longitudinal muscles, even at low stimulus intensity (Figs. 3, 4). This is indeed what was observed in embryonic leeches, before GABAergic inhibition is detectable . The presence of this generalized inhibition means that all the motor neurons--even those that produce the contraction that is the active component of the bending response--normally receive a significant level of inhibition that strongly reduces the excitation triggered by the stimulus. When we monitored the responses of individual motor neurons with intracellular recordings (Figs. 5, 6) we found exactly this: all excitors became significantly more active in the presence of BMI.

Producing scalable neuronal activity appears to be a property of many nervous systems, some much more complicated than that of the leech. For instance, a recent study on the rodent somatosensory cortex suggests that cortical circuits regulate their relative levels of excitation and inhibition across varying magnitudes of input. Combined excitation and inhibition appears to be required for sensory processing not only in the somatosensory cortex, but in visual, auditory, and olfactory systems. The level of inhibitory activity has long been recognized as a determinant of triggering seizure activity, suggesting that a delicate balance of ongoing excitation and inhibition is important for normal functioning of the vertebrate brain. Modeling studies have found, for instance, that for activity to be able to propagate through a structure like the cortex without explosive activation requires a very narrow balance between excitation and inhibition. Our results indicate that even only moderately complex neuronal networks employ a balance between excitation and inhibition to produce useful behaviors.

The issue of gain control has become recognized as one of the most universal neural computational principles. Previous studies had concluded that inhibition produced a linear shift in the input-output function of a neuron (a subtractive process) rather than a change in its slope (a divisive process). It has proven difficult to find cellular mechanisms that can change the gain of a system in a controlled way. For instance, pure inhibition produces a subtraction (i.e., a shift in the input/output function to a less sensitive part of the response range) rather than division (i.e., a decrease in the slope of the input/output function). In general, addition and subtraction are linear processes, whereas multiplication and division are nonlinear ones. Because it produces a nonlinear change in excitatory synaptic inputs, shunting inhibition has been proposed as a mechanism for division, but the effect of having a threshold for spiking acts to offset this nonlinearity and make the input/output function for spiking activity very nearly linear. Another mechanism proposed is modulation of voltage-sensitive channels in the dendrites of cortical neurons by serotonin and norepinephrine because the active dendrites produce a nonlinearity that approximates

multiplication . Another, more systems-level mechanism for producing multiplication, is to balance the overall level of excitation and inhibition so that the membrane potential of the neuron remains constant but the neuron becomes less responsive to a given input as the balanced excitation and inhibition increases .

Feed-forward inhibition has been found, in several systems, to adjust the timing at which spikes occur . Our results show that feed-forward inhibition can also be used to adjust the gain of the circuit that triggers it,. We found that a generalized feed-forward inhibition onto the circuit produces a multiplication of the local bend response over the whole range of stimulus amplitudes, from threshold to saturation (Fig. 2). Our simple model of parallel excitation and inhibition (Fig. 8A) shows that a feed-forward inhibitory circuit, activated in a graded manner by the sensory cells, can change the gain of the local bending circuit, and therefore could explain the results of physiological experiments with GABA blockers (Fig. 2), whereas a saturating inhibitory circuit (Fig. 8B) failed to reproduce the experimental results. It is possible that modulation of this feed-forward inhibitory circuit, represented by G in the circuits of Fig. 8, could be partially responsible for the suppression of the local bend response during other behaviors such as feeding (Misell et al., 1998).

## **EXPERIMENTAL PROCEDURES**

### **Leech care**

Adult medicinal leeches (*Hirudo medicinalis*) from Carolina Biological Supply Co. (Burlington, NC) and Leeches USA (Westbury, NY) were maintained in a cool room (15°C; 12 hour light/dark cycle) in five-gallon aquaria containing Instant Ocean Sea Salt (Aquarium Systems, Mentor, OH; diluted 1:1000 with de-ionized water). They weighed 2.0-5.0 gram and had not eaten for at least four weeks.

## Body wall preparations

To dissect the leeches, we used ice-cold leech saline to anesthetize the leeches. To perform experiments, we used saline at room temperature (20-22°C). Body wall preparations produced reliable local bends for longer than 4 hours. To reduce variability, we always used segment 10 of the 21 midbody segments. We waited at least 3 minutes between stimuli to avoid sensitizing or habituating motor responses. We used body wall preparations similar to those used previously, consisting of three segments removed from the leech midbody region (Fig. 1A) and cut along the dorsal midline. We removed the anterior and posterior ganglia, leaving only the central segment innervated by a single ganglion, then flattened the body wall and pinned it skin-side-up on a plastic Petri dish coated with Sylgard (Dow Corning, Midland, MI; Fig. 1B, C). We used these preparations to record behavioral movements (Fig. 2). To apply drugs to either the ganglion or the body wall selectively, we used a *split body wall preparation*, in which we additionally cut along the ventral body wall, leaving the ganglion attached to the left and right halves (Fig. 3A); we then formed a water-tight Vaseline well around the ganglion through which the lateral nerve roots passed. To record from neurons and stimulate them individually, we used a *hole-in-the-wall preparation*, in which the opening in the ventral body wall was limited to a small hole just over the ganglion (Fig. 4C). For the experiments using voltage-sensitive dyes, we used a single isolated ganglion dissected free of the body wall entirely and pinned to the Sylgard in a Petri dish. In some electrophysiological and all imaging experiments, we removed the connective tissue capsule and the glial packets that encase the neuronal somata to ease cell impalements and to deliver both drugs and voltage-sensitive dyes.

We recorded intracellularly from neuronal somata with sharp glass microelectrodes (20-30 M $\Omega$  filled with 3 M potassium acetate). We identified motor neurons by their location, size, and electrophysiological properties, and delivered current-clamp pulses using an Axoclamp 2-A amplifier controlled with

Axograph 4.9 (Axon Instruments, now Molecular Devices, Sunnyvale, CA) on a PowerPC G3 computer (Apple, Cupertino, CA). We removed all the inhibitory effects produced by the inhibitory motor neurons by passing strong hyperpolarization (-2 to -7 nA) into one inhibitory motor neuron ; this works because all the inhibitory motor neurons are electrically coupled to one another (Fig. 4B)

### **Delivery of GABA blockers.**

Preliminary experiments using bicuculline methiodide (BMI), SR 95531 (“GABAzine”), and picrotoxin showed that only BMI blocked the inhibition from inhibitory motor neurons onto excitatory motor neurons, a synapse known to be GABAergic ; we therefore used only BMI to block inhibitory transmission. BMI is known to block calcium-activated potassium channels responsible for after-hyperpolarization in a variety of mammalian preparations, thereby increasing the excitability of the neurons . We saw no evidence for such effects on leech neurons; in fact, a previous study as well as our own control experiments (in the section on GABAergic Inhibition) found that BMI slightly hyperpolarized leech motor neurons, thereby *decreasing* their excitability. We delivered BMI (Sigma-Aldrich) to the ganglion by a gravity-fed drip system at a concentration of 0.1mM. Initial experiments showed that this concentration produced complete block of the central inhibition among the motor neurons, but did not block the inhibitory neuromuscular junctions in the body wall.

### **Stimulus: force controller**

As described previously , we used a Dual-Mode Lever Arm System (“poker”; Aurora Scientific, Ontario, Canada, Model 300B) to deliver tactile stimuli at a chosen force (0.75-400 mN) to the leech body wall using a 1 mm diameter bead of epoxy on the tip of a 27 ga needle (Fig. 1A). We mounted the head stage of the force controller on a micromanipulator (Narishige International, East Meadow, NY). The

stimuli produced a range of local bend responses similar to the bends produced in earlier studies using smaller forces with smaller-tipped filaments .

## **Terminology**

We have chosen to use the terms “ipsilateral” and “contralateral” to indicate the locations of the peripheral fields of sensory and motor neurons rather than to indicate the locations of their somata within the ganglion. This preserves their functional connectivity: each mechanosensory P (pressure sensitive) cell excites its ipsilateral excitatory motor neuron, even though the somata are on opposite sides of the ganglion. In addition, we use the term “on-target” to refer to the motor neurons that contract the body wall in the *same* area of body wall innervated by the stimulated P cell, and “off-target” to refer to the motor neurons that contract muscles on the body wall directly opposite (Figs. 4A, 5). The areas between these two are called “intermediate” in location. Each longitudinal muscle motor neuron is identified by three features: (1) the location of the longitudinal muscle it innervates (D = dorsal, V = ventral); (2) whether it excites the muscle or inhibits it (E or I); and (3) the number assigned to its soma on the standard ganglionic map . Hence, cell DI-1 inhibits dorsal longitudinal muscles and its soma is in map location 1. For brevity, we sometimes use the terms “excitor” and “inhibitor” in place of “excitatory longitudinal muscle motor neuron” and “inhibitory longitudinal muscle motor neuron.”

## **Behavioral video recordings**

We recorded the image of the body wall preparation (Fig. 1B, C) through a Wild dissection microscope using a C-Mounted Hitachi KP-M1 monochrome CCD camera (Image Labs International, Bozeman, MT). We captured the images (640x480 pixel resolution) at 10 Hz and digitized using a Data Translation frame grabber card (DT3155) controlled with the MATLAB (The Mathworks, Natick, MA)

Image Acquisition Toolbox on a PC computer (Fig. 1A). On a different computer, pulses from Axograph 4.9 software (Axon Instruments, Union City, CA) synchronized video acquisition with the stimulus controller and the electrical recordings. As previously described, we tracked the body wall motion by making optic flow estimates between successive image frames. We captured 20-40 images that include the onset of the bend, then calculated optic flow fields between successive frames.

To minimize the effects of restraining the preparation in behavioral studies, we pinned the body wall only in the denervated anterior and posterior ends (Fig. 1B). In these preparations, we measured local bending responses along anterior-posterior lines in the five innervated annuli at four locations: on-target ventral ( $V_{on}$ ), and three off-target sites: ventral ( $V_{off}$ ), lateral ( $L_{off}$ ), and dorsal ( $D_{off}$ ). (The lateral and dorsal movements ipsilateral to the stimulus were distorted by the movements of the stimulator arm and could not be measured reliably.) We manually marked points along the edges of the five annuli corresponding to the innervated segment in the first frame of each of the resulting movies, then used the optic flow detection algorithm to track the motion of these markers. We delivered mechanical stimuli of 3-second duration spaced 3 minutes apart to prevent response adaptation. The actual force applied was verified using a lab balance placed under the petri dish. In this manner, forces as low as 1 mN could be applied with better than 10% reproducibility.

To record electrophysiologically, we needed to pin the preparation tightly along all four of its margins (Fig. 1C). The contractions at the site of stimulation were readily visible; they were smaller than those recorded in less constrained preparations but were qualitatively similar. The relaxations contralateral to the site of stimulation, however, were often not visible. To measure local bending in these preparations, we selected a rectangular region of interest (ROI) that showed robust movement and was free from edge or pinning artifacts (Fig. 1C). The ROI spanned 1-2 annuli along the long axis of the leech and included its entire circular axis. For a given preparation, we used the same ROI for all trials. Because we were most

interested in the contribution to local bending produced by the longitudinal muscles, we calculated only that component of the movement that ran parallel to the leech's long axis.

### **Quantification of behavior**

In the loosely-pinned preparations (Fig. 1B), we compared the distance between anterior and posterior markers 0.5 seconds after withdrawal of the stimulator to the distance just before stimulation. The recording below the trace is one smoothed response to a stimulus at  $V_{on}$  in the middle of the intensity range used, with the length measurement normalized to the average length of an annulus (annuli are elevations in the skin of the body wall that run circumferentially around the body; five annuli constitute one segment). In the tightly-stretched preparations (Fig. 1C), the stimulus lasted 0.5 seconds and the response peaked at about 1.0 seconds after stimulus offset; we therefore used the cumulative motion profile at the peak of the response, in units of annulus widths. We smoothed these motion profiles with a Gaussian filter. We measured the magnitude of the responses as their peak amplitudes because, although it is only a single measure of each response, it is the closest behavioral counterpart to the peak firing rate of the motor neurons responsible for longitudinal muscle contractions .

### **Monitoring the electrical activity of multiple neurons using voltage-sensitive FRET dyes**

We stained dissected, isolated ganglia from adult leeches with a pair of FRET dyes: 10  $\mu$ M solution of the donor, coumarin (*N*-(6-chloro-7-hydroxycoumarin-3-carbonyl)-imyristoylphosphatidylethanolamine)) and 12.5  $\mu$ M of the acceptor, oxonol (bis (1,3-diethyl-thiobarbiturate)-trimethine oxonol), both from Vertex Pharmaceuticals Inc., San Diego, CA. For details of their preparation and application, see Cacciatore et al. (1999) and Taylor et al. (2003). We acquired fluorescence images using an upright microscope (Axioskop 2FS; Zeiss, Thornwood, NY) equipped with

a 40 X, 0.8 NA water-immersion objective (Achromplan; Zeiss). For epi-illumination we used a tungsten halogen lamp (64625 HLX; Osram Sylvania, Danvers, MA) in standard housing (HAL 100; Zeiss), powered by a low-ripple power supply (JQE 15-12M; Kepco, Flushing, NY). For all voltage-sensitive dye imaging, we acquired images only at the coumarin emission wavelength. The filter set consisted of a  $405 \pm 15$  nm bandpass excitation filter, a 430 nm dichroic mirror, and a  $460 \pm 25$  nm bandpass emission filter (Chroma Technology Corporation, Brattleboro, VT). We acquired the optical data using a water-cooled CCD camera (MicroMax 512 BFT; Roper Scientific, Tucson, AZ) operated in frame-transfer mode at a frame rate of 20 Hz. The CCD chip in this camera has 512 X 512 pixels, but we binned at 4 X 4 pixels to yield a 128 X 128 pixel image. The CCD chip was maintained at  $-25^{\circ}\text{C}$  during imaging. Images were stored using the software package Win-View/32 (Roper Scientific, Trenton, NJ). The combination of coumarin and oxonol yielded sensitivities of 5–20% change in fluorescence/100mV for 1Hz square-wave voltage signals with a 10 mV amplitude, centered around a resting potential of -50 mV.

### **Image analysis.**

We analyzed the images using a custom-made graphic user interface in Matlab. We averaged all pixels within each cellular outline in each frame . To find neurons responding to a stimulated mechanosensory neuron, we impaled the sensory neuron's soma with a microelectrode and passed a train of current pulses (4nA, 7ms, 15Hz) for 500 milliseconds each second while simultaneously collecting images at 20 Hz for 10 seconds. We always impaled a postsynaptic cell to compare optical data with intracellular recordings. Using coherence analysis (coherence is essentially a correlation of two trajectories at the dominant shared frequency, in this case 1 Hz), we identified neurons whose optical signals were correlated with the stimulated one . In some experiments, a 100  $\mu\text{M}$  BMI solution was

applied to the ganglion; images were taken before and during BMI application. We then washed out the BMI solution for 10 minutes and obtained a post-wash recording.

### **Statistics.**

We applied standard statistical tests to our data (one-way ANOVA, a posteriori Tukey test; MANOVA for multivariate data, and corrected one-tailed and two-tailed t-tests where appropriate) using the Statistics Toolbox in MatLab. All values listed are mean  $\pm$  SEM.

### **Modeling input-output functions of the neurons in the local bend circuitry.**

The P cell in the model was activated by skin touch using a sigmoidal of the form:

$$P(F) = 1/2 + 1/2 \tanh(\alpha_P \log(F / \theta_P)),$$

where F is the touch force (in milliNewtons),  $\theta_P = 25$  mN, and  $\alpha_P = 0.3$ .

The activation of the other cells was modeled using sigmoidal functions of their synaptic inputs:

$$G(P) = 1 / (1 + (\theta_G / P)^{\alpha_G}),$$

$$I(P, G) = 1 / (1 + (\theta_I / (P + \gamma G))^{\alpha_I}) + I_0,$$

and

$$M(I) = 1 / (1 + (\theta_M / I)^{\alpha_M}).$$

To match the experimental results (black curves in Fig. 8A), we used ( $\theta_G = 1.4$ ,  $\alpha_G = 1.7$ ,  $\theta_I = 0.4$ ,  $\alpha_I = 1.1$ ,  $I_0 = 0.02$ ,  $\theta_M = 1.4$ ,  $\alpha_M = 1.9$ , and  $\gamma = 1.65$ ).

### **ACKNOWLEDGEMENTS**

We thank our colleague, Massimo Scanziani, for helpful suggestions in preparing the manuscript. The research was supported by an NIH research grants MH43396 and NS35336 (W.B.K.) and by gifts from the Microsoft Research Laboratory and Richard Geckler.

**REFERENCES**

## FIGURE LEGENDS

**Figure 1.** Generating and recording local bending responses. **A.** Schematic diagram of a leech, indicating the location of its central nervous system: head and tail brains (depicted as large dots at anterior and posterior ends) with 21 segmental ganglia (smaller dots) in the ventral nerve cord. To record local bending, we cut open the body wall of segments 8–12 along the dorsal midline and pinned it down, outside up, on a Sylgard substrate. This creates a flat piece of body wall with the cut dorsal midline at the lateral edges. We removed ganglia 8, 9, 11, and 12, leaving only ganglion 10 connected to the body wall. We recorded movements from above using a CCD camera mounted on a dissecting microscope, digitized the images, and stored them on a computer. We delivered mechanical stimuli using an electronically controlled poker with a surface area of about 1 mm<sup>2</sup>. The duration of each stimulus was either 3 seconds (Fig. 2) or 0.5 seconds (all other experiments); stimuli were spaced 3 minutes apart to prevent response adaptation. **B.** Loosely pinned preparation used to generate local bending. We manually chose points along the edges of the five annuli corresponding to the innervated segment in the first frame in each of the movies (the most anterior and posterior points are indicated by arrows), and used an optical flow detection algorithm to track the motion of these markers. The distance between the anterior and posterior markers 0.5 seconds after withdrawal of the stimulator was compared to the distance just before stimulation. The trace below the body wall image is a smoothed version of the change of distance between the anterior and posterior markers at each of 4 locations at 0.5 seconds after withdrawing the stimulus.  $V_{on}$  is the on-target ventral location of the stimulus;  $V_{off}$ ,  $L_{off}$ , and  $D_{off}$  are off-target locations in ventral, lateral, and dorsal locations whose movements we plotted. The distance moved was initially measured in units of pixels, which were then normalized to annuli by measuring the number of pixels per annulus. **C.** Tightly pinned preparation used to record local bending and neural activity. We measured movements in a selected

region of interest (ROI) away from the stimulus site (arrow), to avoid optical and mechanical artifacts caused by movements of the poker. The ROI is indicated as a dark swath across the middle of the image. We represented movements of 80-240 locations in a grid within the ROI as vectors. We averaged the lengths of the vector components parallel to the long axis of the body wall at 20-80 locations and smoothed this result to obtain a bend profile (graph below the body wall image). Again, the magnitudes of the movements were normalized to number of annuli.

**Figure 2.** The effects of GABAergic inhibition on the magnitude of local bend responses. **A.** Responses of the on-target contractions in the ventral body wall to mechanical stimulation at a single mid-ventral site in normal saline (filled circles) and in saline with 0.1 mM BMI (open circles). The black solid line is a sigmoid fit of the responses in saline, the dashed line is the sigmoid fit to the responses in BMI, and the grey line is the black line multiplied by 2.1. The remaining three graphs are similar plots from responses recorded at three different contralateral off-target sites: ventral (**B**), lateral (**C**), and dorsal (**D**); the grey lines are the black lines multiplied by -1.0 (**B**), 0.2 (**C**), and 0.5 (**D**). In all graphs, the magnitudes of the movements were normalized to number of annuli. All experiments were repeated in 10 preparations.

**Figure 3.** Bath-applied BMI blocks GABAergic inhibition centrally, not peripherally. **A.** Using a split body wall preparation (icon) with a Vaseline wall around the ganglion, we delivered mechanical stimuli at a single location (left lateral edge) and a single intensity (200 mN). We measured the bend profiles before adding BMI (Control), after adding BMI to the saline bathing the body wall (BMI Periphery), after adding BMI to the saline bathing the ganglion (BMI Central), and after replacing the BMI with saline (Wash) after each BMI addition. This example shows a strong contraction on the side stimulated and a weak contraction on the opposite side. When BMI was applied, the on-target response nearly doubled in size and the off-target response became nearly as large as the on-target response. The fact that there is no

contraction in the middle of the graph is an artifact of the preparation: the body wall was split up the ventral midline to provide access to the ganglion; the optic flow algorithm detected no movement in this region. We measured on-target and off-target amplitudes at the peaks, which were in sites minimally affected by the mid-ventral incision. **B.** Quantification of the BMI effects on the ganglion and on the body wall (n = 10). Adding BMI to the saline bathing only in the body wall (BMI Peripheral) did not change either the on-target or the off-target response, whereas adding BMI to the saline bathing the ganglion (BMI Central) produced a significant increase in both the on-target and off-target responses compared either to pre-BMI application conditions (Saline) or after washing out the BMI (Wash)(ANOVA,  $p < 0.001$ ; post hoc t-tests for individual comparisons  $p < 0.01$ ).

**Figure 4.** Removing inhibition among motor neurons by hyperpolarizing the inhibitors increased the off-target response but did not affect the on-target peak amplitude. **A.** Simplified version of the local bend circuitry . Just four pressure-sensitive mechanoreceptive neurons (a  $P_D$  and a  $P_V$  on each side) innervate overlapping regions of the skin, with the centers of their receptive fields in the middle of the two dorsal (D) or ventral (V) regions. All four P cells excite a collection of local bend interneurons (LBIs), which in turn excite the motor neurons to the longitudinal muscles. There are two functional types of motor neurons, excitatory (E) and inhibitory (I) that innervate either the dorsal (D) or ventral (V) longitudinal muscles. All identified connections are feed-forward and excitatory, except for those made by the inhibitory motor neurons, which make GABAergic inhibitory synapses onto both the appropriate longitudinal muscles and the corresponding excitatory motor neurons. Hence, there are four types of motor neurons (DE, DI, VE, and VI) on each side. (The somata of all neurons are in a ganglion on the ventral surface of the segment; they are shown in the middle of the body in this diagram for clarity.) Motor neurons causing muscle contractions in the quadrant whose P cell was stimulated are “on-target”

and the ones on the side opposite to the stimulation are “off-target”. **B.** Schematic version of the electrical connections among the inhibitory motor neurons. Because they make non-rectifying electrical connections to one another, hyperpolarizing one inhibitor hyperpolarizes all of them. (Not shown: DE cells make non-rectifying electrical connections to other DEs, and VEs make non-rectifying electrical connections to other VEs; these connections are not represented in either diagram.) **C.** We used the hole-in-the-wall preparation (icon) to impale inhibitory motor neurons while eliciting local bending. We stimulated a single site (black dot on the x-axis) and a single intensity (200 mN) while strongly hyperpolarizing a single inhibitor, thereby inactivating all the inhibitory motor neurons via widespread electrical connections. Mean bend profiles are shown for one preparation before (solid black line) and while (grey solid line) passing  $-2$  to  $-7$  nA of hyperpolarizing current into an inhibitory motor neuron. **D.** The peak amplitude of the on-target responses were not affected by hyperpolarizing the inhibitory motor neurons ( $p > 0.40$ ), whereas the off-target responses were significantly increased by these hyperpolarizations ( $p < 0.04$ ).

**Figure 5.** Effects of bicuculline methiodide (BMI) on the responses of longitudinal excitatory motor neurons (DEs and VEs) to P cell stimulation. In panels **A** through **D**, the top traces show the times when spikes were generated in the right  $P_v$  neuron; the middle traces are intracellular recordings from either a DE or a VE; and the bottom traces are voltage-sensitive dye recordings obtained from the motor neuron simultaneous with the intracellular recording just above it. The VSD units are percent change in amplitude of the fluorescent signal ( $\Delta F/F \times 100\%$ ). In every panel, the traces on the left were obtained while the ganglion was bathed in standard saline and the traces on the right (against a grey background) were obtained from the same neuron after replacing the saline with one containing 0.1 mM BMI. **A.** Intracellular and VSD recordings from the contralateral cell DE-3, an off-target excitor of left dorsal longitudinal muscles. **B.** Intracellular and VSD recordings from the ipsilateral cell DE-3, an intermediate

excitor of right dorsal longitudinal muscles. **C.** Intracellular and VSD recordings from the contralateral cell VE-4, an intermediate excitor of left ventral longitudinal muscles. **D.** Intracellular and VSD recordings from the ipsilateral cell VE-4, an on-target excitor of the right ventral longitudinal muscles.

**Figure 6.** Effects of bicuculline methiodide (BMI) on the responses of all neurons on the dorsal surface of a mid-body ganglion. **A.** Images of the dorsal surface of a midbody ganglion used to record neuronal activity with voltage-sensitive dyes. Hand-drawn ellipses indicate the boundaries of neuronal somata. The numbers were assigned according to the positions of the somata on a standard ganglionic map (Muller et al., 1981). The colors indicate the phase of the VSD trajectories of each neuron relative to the stimulus burst cycles, as determined by the phase plots in E1-E3 below. The arrows here and in panels **C**, **D**, and **E** identify the cell DE-3 that was recorded intracellularly. Scale bars: 50 $\mu$ m. **B.** The top traces are intracellular recordings from a P<sub>v</sub> cell (outside the field of view in panel A) showing when trains of 5 action potentials were evoked by depolarizing current pulses (5nA, 7 ms, 10 Hz) generated for 500 ms at 1 Hz. Simultaneous intracellular recordings (middle traces) and optical trajectories (bottom traces) show the responses of the indicated cell DE-3. The colors of the optical traces correspond to the phases of the response (from panel **E**): blue indicates inhibition and gold indicates excitation. The B2 recordings are responses of DE-3 to the same P<sub>v</sub> stimulation with 0.1 mM BMI in the bathing solution. **C.** Recordings of the driven spike burst in the P<sub>v</sub> cell (top trace) along with fluorescence signals from the 43 cells visible in the ganglion (**A1-A3**). Colors of the fluorescence traces correspond to phasing of the responses (from **E1-E3**); grey traces indicate non-coherent neurons. Calibration bars are displayed below and to the right of the recordings. Signals are lined up in decreasing order of their coherence values, with the maximum value (with the largest oscillation amplitude) at the top. **D.** Optical recordings from the same 43 neurons, with response valence indicated by color: red indicates depolarization to each burst and blue indicates

hyperpolarization to each burst (color bar to the right of **A3**). Traces with no responses to the stimuli are grey. **E.** Polar plots indicate the coherence phase (circumferential distance from  $0^\circ$ ) and magnitude (linear distance from the center of the plot) for all neurons observed in the image. Each point indicates the average phase and maximal amplitude of a single neuron; the lines from each point indicate the standard errors in both amplitude and phase about the mean. Neurons with amplitude values greater than the dashed line are coherent with the stimulus at the 95% confidence limit.

**Figure 7.** Effects of removing inhibition, by hyperpolarizing the inhibitors responses, on all neurons on the dorsal surface of a mid-body ganglion. **A.** Images of the dorsal surface of a midbody ganglion used to record neuronal activity with voltage-sensitive dyes. As in Fig. 2, we impaled a mechanosensory  $P_V$  neuron (outside the field) and elicited a train of spikes at 10 Hz for 500 ms, repeated every second for 10 seconds. The color of each neuron indicates the phase of its response relative to the stimulated neuron (**C1-C3**). Experiments were performed without passing current into the DI-1 neuron (Control), during the time that cell DI-1 was hyperpolarized with -5 nA, then again not passing current into DI-1. Scale bars: 50 $\mu$ m. Arrows point to cell VE-4, an excitatory motor neuron to the ventral muscles, which is inhibited by VI-1 in standard saline. The arrows in succeeding panels indicate data from this motor neuron. **B.** Raster plots showing the optical signals from all circled cells in **A**, with changes in fluorescence amplitude indicated by colors (calibration bar to the right of the raster plots). **C.** Polar plots showing the coherence phase (the angle from  $0^\circ$ ) and magnitude (distance from the center) of the responses of all observed neurons. Values greater than the dashed line are coherent, at 95% confidence, with the stimulus. **D.** Number of neurons that showed significantly coherent responses to stimulation of a  $P_V$  cell relative to the total number of cells imaged in each experiment (mean  $\pm$  SEM for control): pre-manipulation control (n =

13), after adding BMI ( $n = 7$ ), while hyperpolarizing the inhibitors ( $n = 6$ ), and after each manipulation ( $n = 13$ ). (\*  $P < 0.05$ , \*\*\*  $P < 0.001$  (One-way ANOVA,  $F_{3,33} = 12.11$ , a posteriori Tukey test)).

**Figure 8.** Modeling the influence of central GABAergic inhibition on the local bend response. **A.** Model with feed-forward inhibition. **A1.** Schematic of the modeled circuit. The model consists of one somatosensory P cell (P), one interneuron (LBI), one motor neuron (MN) and one GABAergic inhibitor (G). The T-bars indicate excitatory connections and black circles represent inhibitory connections. **A2.** Activity of the modeled cells as a function of skin touch: with inhibition intact (solid black), with inhibition blocked (dashed black), with decreased inhibition (down-pointing triangles), and with increased inhibition (up-pointing triangles). For the black curves, the model parameters (slopes, locations of half-maximum response, and synaptic strengths) were chosen to make the output resemble the experimental results (grey lines in bottom panel: control, solid; with BMI, dashed). **B.** Model with saturating inhibition. **B1.** Schematic. The thick T-bar represents a stronger synapse between P and G. All other connections were the same as in A. **B2.** Activity of the modeled cells: with a medium amount of saturating inhibition (solid), increased inhibition (up-pointing triangles), reduced inhibition (down-pointing triangles), and no inhibition (dashed; identical to results in A2 by construction). In this version of the model, increasing the activity of the G cell shifted the MN output left to right (solid lines in LBI and MN), unlike the experimental data (grey lines as in A2).

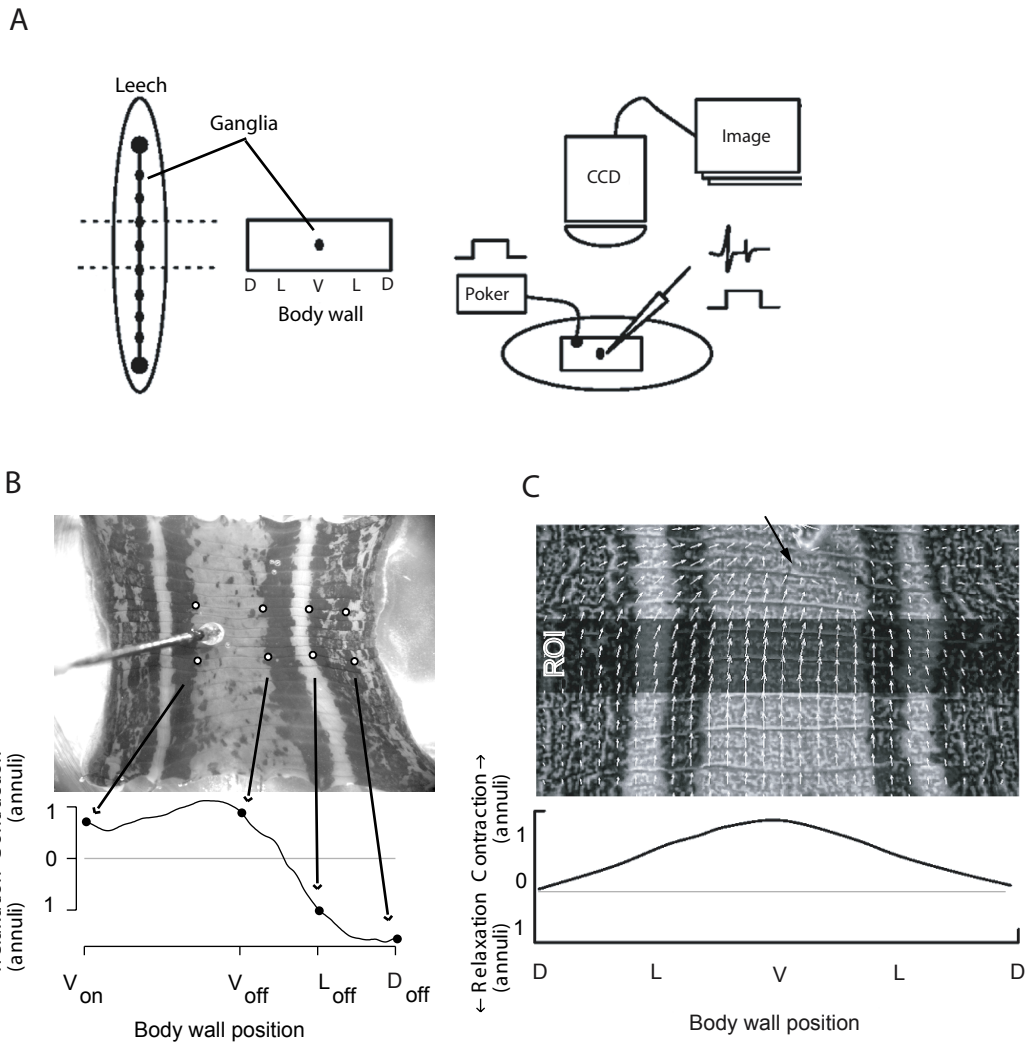


Figure 1

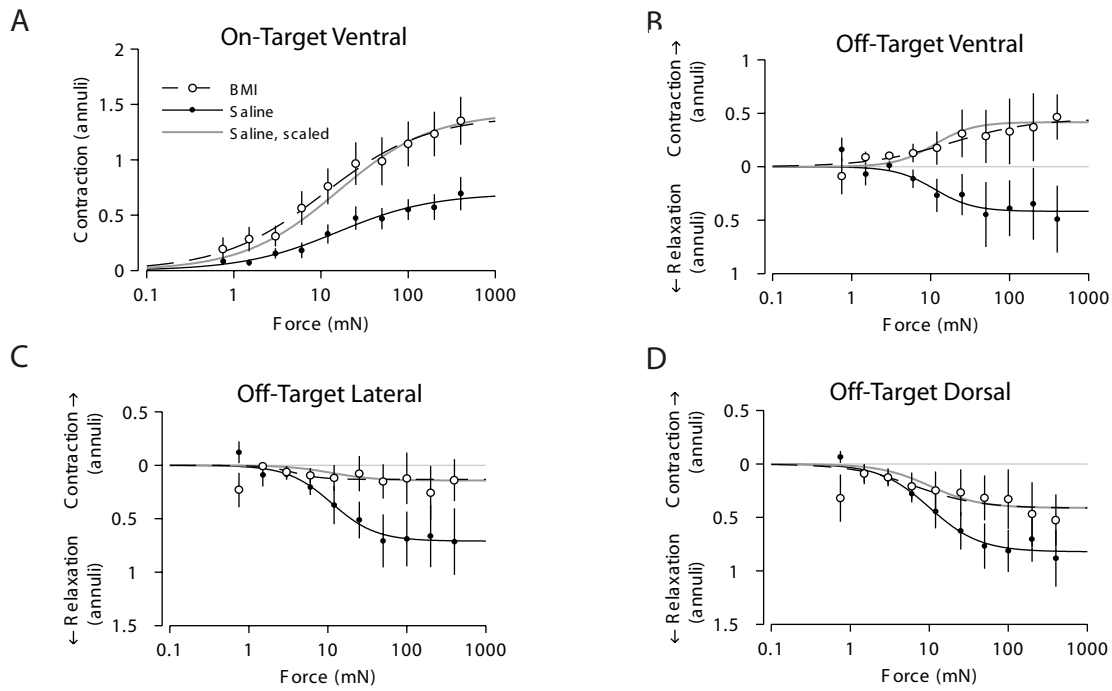


Figure 2

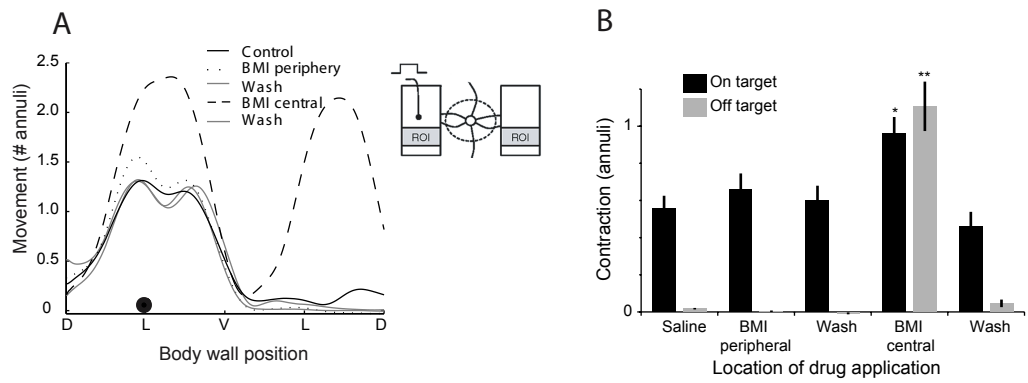


Figure 3

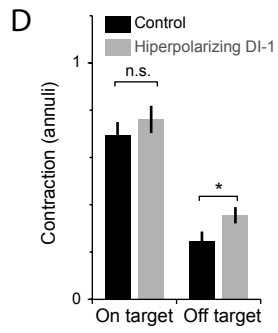
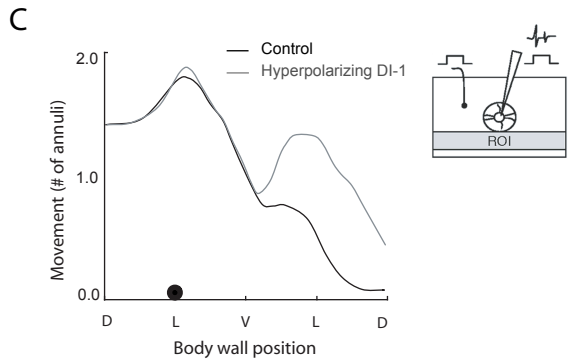
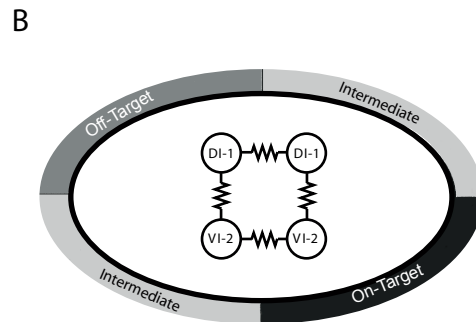
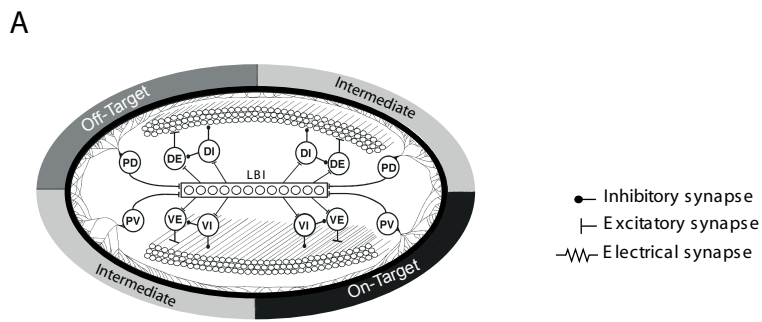


Figure 4

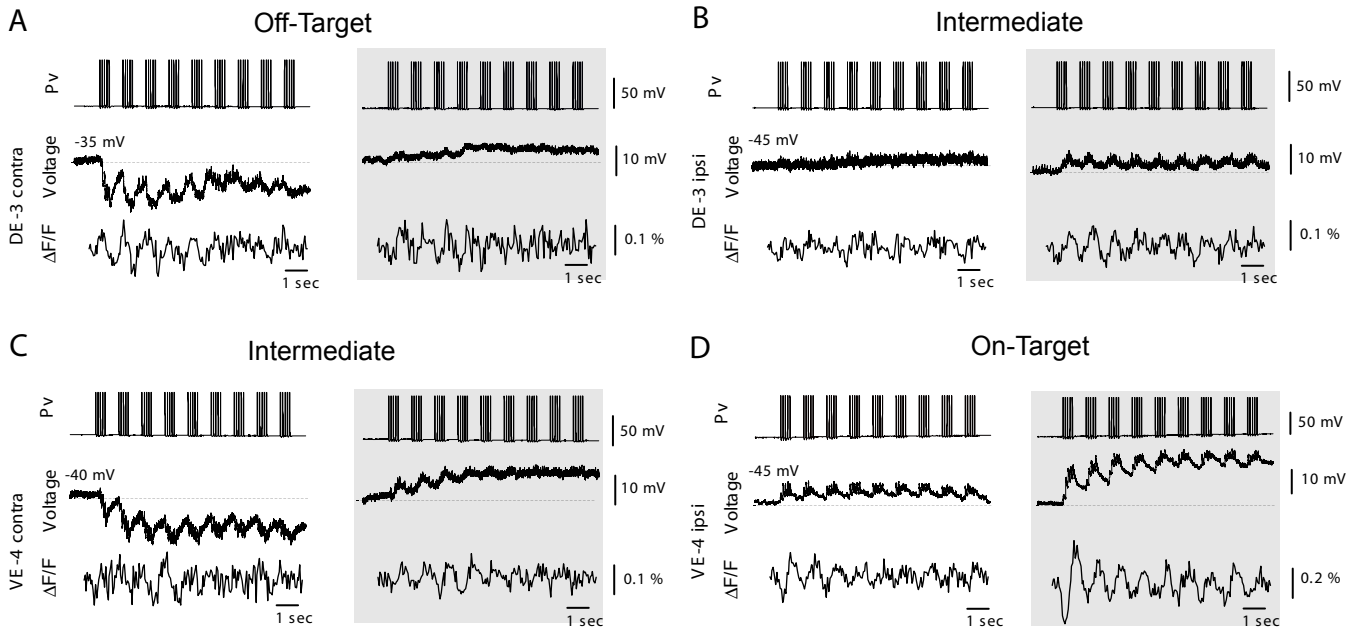


Figure 5

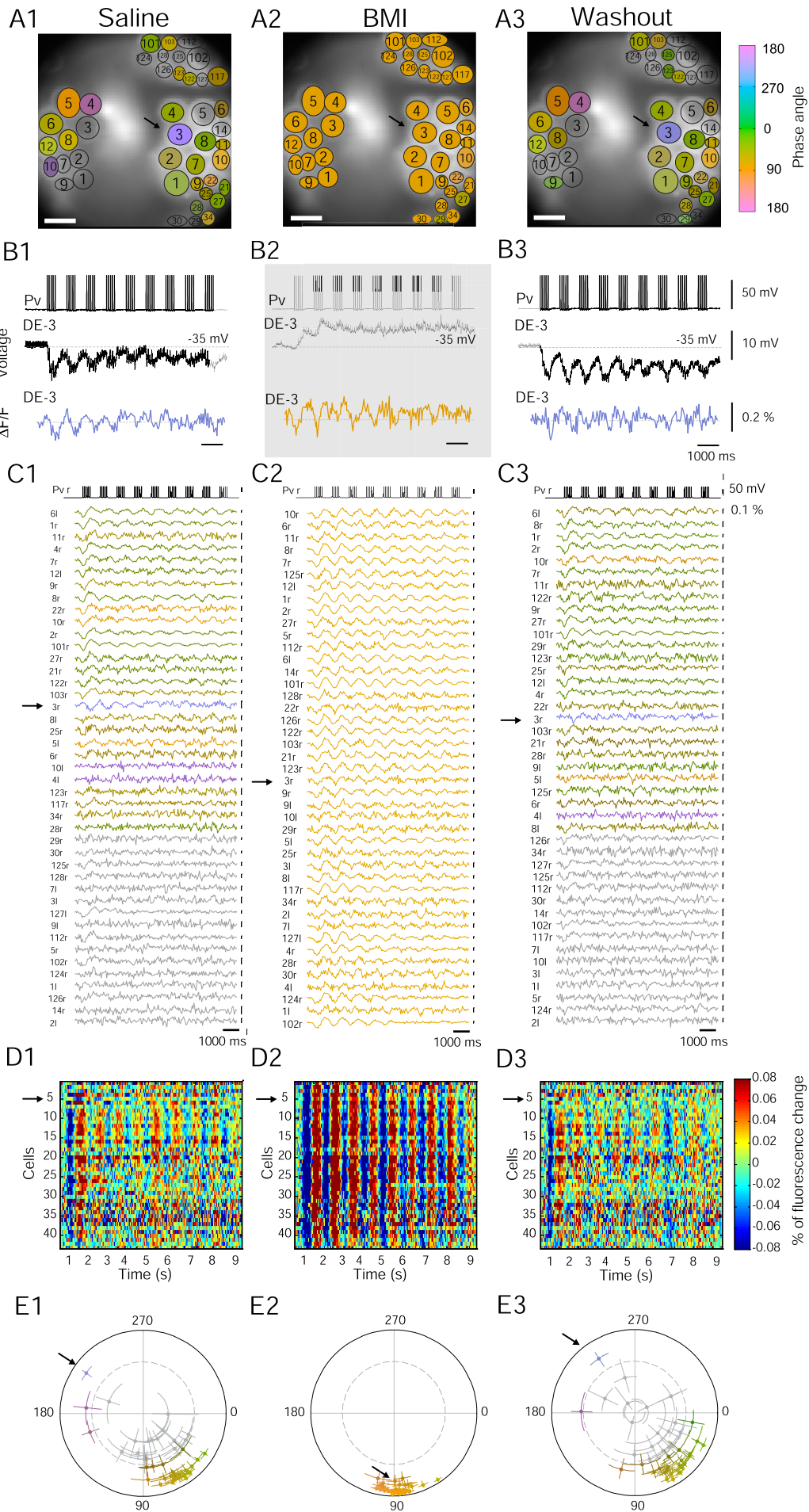


Figure 6

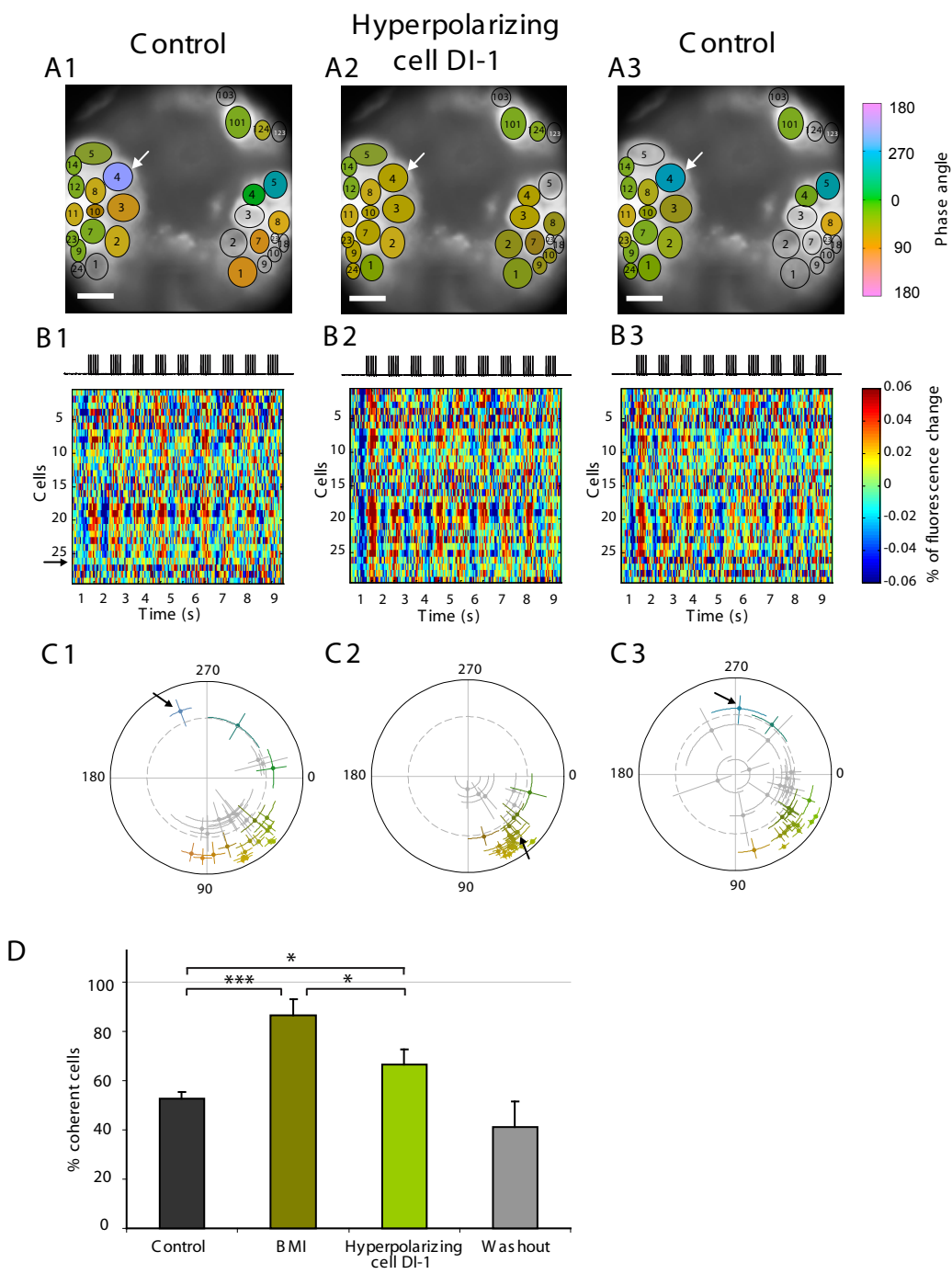


Figure 7

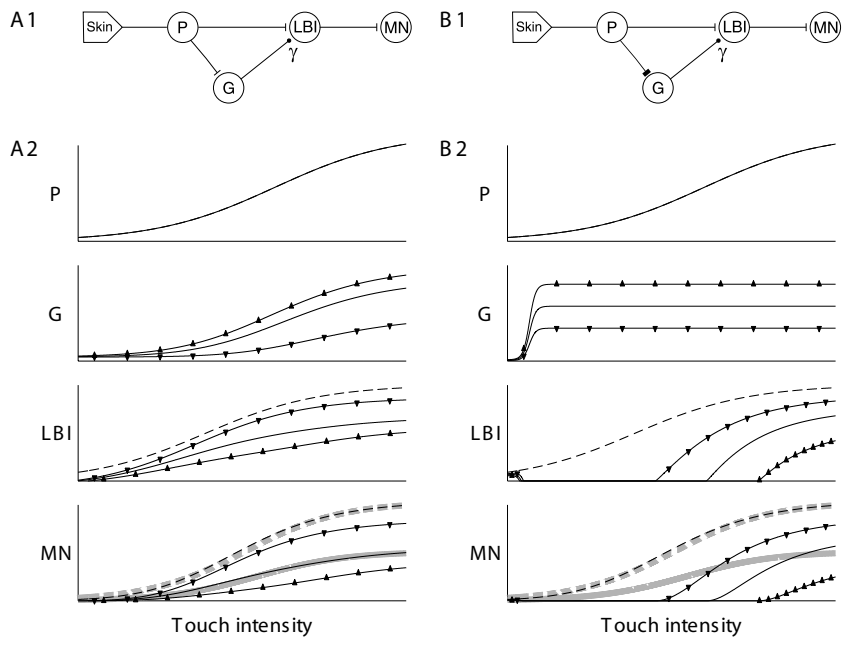


Figure 8